On The Electrotonic Spread in Cardiac Muscle of the Mouse

ICHIRO TANAKA and YUTAKA SASAKI

From the Department of Physiology, Tokyo Women's Medical College, Tokyo, Japan

ABSTRACT As an appropriate model which can simulate the cardiac working muscle with respect to the passive electrical spread, a lattice whose sides have linear cable properties is presented, and the passive potential spread on the model is mathematically analyzed in the fiber direction. Distribution of electrotonic potential in the fiber direction was measured with a pair of intracellular microelectrodes in the cardiac muscle fiber of mouse. By employing "pencil type" microelectrodes potential distribution in the transverse direction within a fiber was also measured. This transverse effect was differentiated from the longitudinal potential distribution. A tonically applied potential at any point of a cell interior spreads continuously in a manner described by a Bessel function. Using appropriate electrical and morphological parameters the experimental results proved to fit the curve obtained from numerical calculation on the model. The apparent length constant obtained for smaller distances (less than 100 μ) from the current source was 70 μ, and it increases as the distance becomes larger. At a point inside the fiber the resistance to the extracellular fluid ranged from 200 to 600 KΩ. The influence of coupling resistance between current and recording electrodes on the measurement of electrotonic potential was examined for small interelectrode distance.

INTRODUCTION

It is a well known fact that the cardiac muscle fibers make complicated anastomoses with each other. This makes analysis of the tissue electrical properties very difficult compared with nerve and skeletal muscle fibers.

Attempts, however, have been made to apply linear cable analysis to cardiac muscle, for example, to the false tendon which has less branched, i.e. relatively linear cablelike features (Weidmann, 1952), and to the terminal Purkinje fiber as an equivalent linear cable consisting of several component fibers attached side by side (Matsuda, 1960).

Working on the rat atrium, Woodbury and Crill (1961) proposed a planar model for the cardiac tissue. They showed theoretically and experimentally that the spatial distribution of a tonically applied potential at any point of a cell interior in the tissue can be mathematically expressed by a Bessel function.

On a morphological basis, however, their model is too simple to simulate the real cardiac tissue.

In the present paper, another model is presented, and its validity will be examined from the theoretical and experimental point of view. For passing current and recording potential, a pair of intracellular microelectrodes and a "pencil type" microelectrode (Tomita and Kaneko, 1965) were used.

In connection with this, effective resistances characteristic of the structure of the anastomosis will also be mentioned. Finally, some experiments were done on the influence of coupling resistance between current and recording electrodes for an exact interpretation of experimental data.

THEORY

I. *Symbols and Nomenclature*

a diameter of the component fiber (cm).

d internodal distance of the syncytium (cm).

n order of nodal point counted from a node at which the current is applied.

N number of fibers between $(n-1)$th to nth nodal points $(=4n)$

R_i specific resistance of the myoplasm of the fiber ($\Omega \cdot$cm).

R_m transverse resistivity of membrane ($\Omega \cdot \text{cm}^2$).

r_i resistance of the component fiber per unit length (Ω/cm).

r_m transverse resistance per unit length of the component fiber membrane ($\Omega \cdot$cm).

λ length constant characteristic of the component fiber $(=\sqrt{r_m/r_i})$ (cm).

x distance along the fiber from the point at which the current is applied (cm).

E_0 produced potential inside the fiber at $x = 0$ when the current, I_0, is applied (the steady state) (v).

E electrotonic potential inside the fiber at x (the steady state) (v).

$E_{n \text{ to } n+1}$ electrotonic potential inside the fiber for the internodal portion between nth and $(n+1)$th nodal points (the steady state) (v).

I_0 applied current, total current through the membrane (the steady state) (amp).

I axial current inside the fiber at x (the steady state) (amp).

R_c characteristic resistance of the component fiber $(=\sqrt{r_i \cdot r_m})$ (Ω).

R_0 effective resistance at $x = 0$, i.e. resistance at $x = 0$ to the large indifferent electrode immersed in the medium $(= E_0/I_0)$ (Ω).

k ratio of R_c to R_0 $(= R_c/R_0)$.

The following symbols are applied when the descriptions of "tip resistance" are given.

c tip radius of micropipette used as current electrode (cm).

ρ specific resistance of the medium in which the current electrode is immersed ($\Omega \cdot$cm).

L distance from the tip of the current electrode (cm).

R_t coupling resistance between current and recording electrode (Ω).

$R_{t(L=0)}$ tip resistance; i.e., value of R_t when distance between both electrodes is 0 (Ω).

II. *Model and Its Mathematical Presentation*

The present model of the ventricular syncytial network is a lattice of practically infinite extent which is provisionally assumed to be of two dimensional spread (see Fig. 1).

Each side of the lattice is a component fiber with linear cable properties. The component fiber is a uniform cylinder of diameter a and length d, which has a uniform internal resistivity R_i and leakage resistance R_m per unit area, with parallel capacitance. Each nodal point represents an anastomosis of cardiac muscle fibers. It is assumed that the thickness of the insulating membrane is uniform and negligible compared with the diameter and that the whole model is in a volume conductor with negligible resistivity.

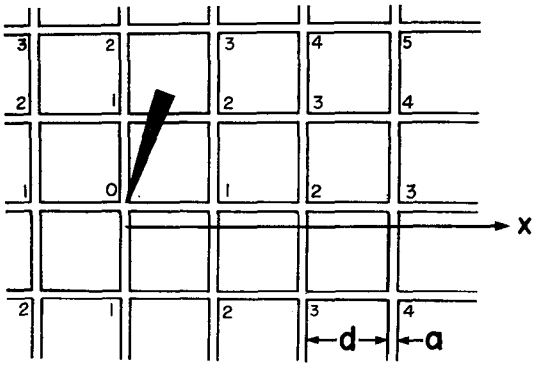

FIGURE 1. Schema of the lattice model. Arrow, current electrode. Numbers, order of nodal point. a, diameter of the component fiber. d, internodal distance. x, distance along the fiber from the tip of current electrode. (See text.)

Under such circumstances the current I_0 is applied across the insulating membrane at a point inside the fiber and the internal distribution of the tonic potential is analyzed against the distance x along the longitudinal axis of the fiber. For the steady state the following differential equation is assumed to hold between the potential E and distance x under a certain condition (see Appendix, section I)

$$\frac{d^2E}{dx^2} + \frac{1}{x} \cdot \frac{dE}{dx} - \frac{1}{\lambda^2} \cdot E = 0 \tag{1}$$

The solution of Equation 1 for the present model is a zero-order modified Bessel function of the second kind

$$E = AK_0\left(\frac{x}{\lambda}\right) \tag{2}$$

where $\lambda^2 = r_m/r_i$ and $A = E_0/m$, where E_0 is the potential at $x = 0$, and m is expressed as follows (see Appendix, section II)

$$m = K_0\left(\frac{\alpha}{\lambda}\right)$$

in which α is a constant depending upon the values of d and λ having a dimension of distance. E has a value of E_0 at $x = \alpha$ in Equation 2.

In order to obtain the morphological parameters of the cardiac muscle of mouse, the length of internodal distances and diameters of the fibers of the epicardial side were measured under the microscope. Their values are shown in Fig. 2. Peak values of a and d were 10 μ and 100 μ respectively.

As for the primary electrical constants of the fiber, information is available

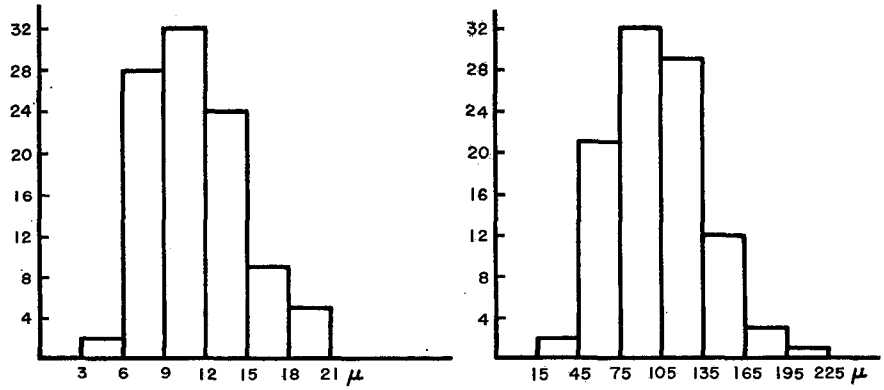

FIGURE 2. Histograms showing the distribution of diameters and internodal distances of epicardial fibers of mouse ventricle obtained from 100 observations. Left, distribution of diameter. Right, distribution of internodal distance.

for mammalian hearts (Weidmann, 1957), but the values adopted in the present paper are, $R_m = 1000\ \Omega\cdot\text{cm}^2$ and $R_i = 100\ \Omega\cdot\text{cm}$, for the simpler calculation. Thus the membrane resistance per unit length of the component fiber, r_m, is $3.18 \times 10^5\ \Omega\cdot\text{cm}$, the internal resistance of the fiber per unit length, r_i, is $1.27 \times 10^8\ \Omega/\text{cm}$, hence the length constant, λ, is calculated to be 0.05 cm.

Using these parameters Equation 2 is graphically presented in Fig. 3. The abscissa indicates the distance in millimeters, and the ordinate shows the values of $\log E/E_0$. The curve is very steep and concave for the distance close to the origin. The tonic potential falls off rapidly in comparison with the exponential decay. For the relatively large values of x, this concavity is very small and is regarded as linear with a length constant of λ.

The relation between the potential distribution and the distance expressed by Equation 2 might well be applicable to that obtained by experiments. For the present model, however, only the nodal points lie strictly on the curve

in Fig. 3 and each internodal portion would have linear cable features. Thus the potential distribution of the internodal portion is generally expressed as

$$E_{n\sim n+1} = A_n \exp\left(-\frac{x}{\lambda}\right) + B_n \exp\left(\frac{x}{\lambda}\right) \tag{3}$$

where A_n and B_n are constants depending upon d, λ, and the order of the nodal point n.

For relatively small values of x, the curve in Fig. 3 is enlarged as shown in

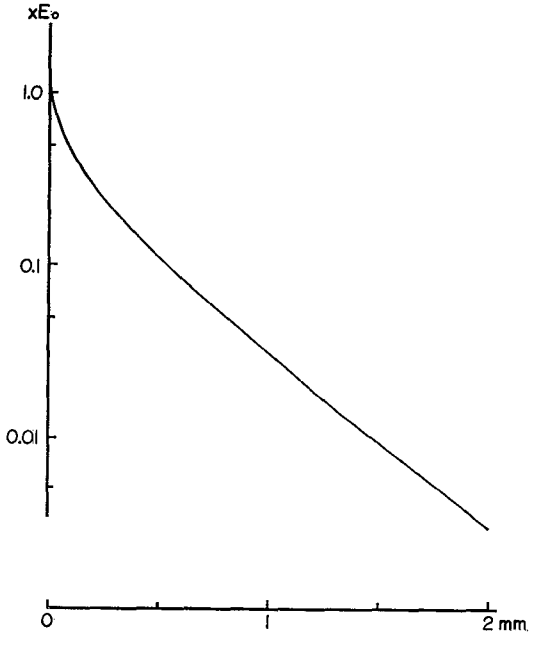

FIGURE 3. Theoretical distribution of the tonic potential along the axis of the fiber. Ordinate, tonic potentials indicated as times of applied potential E_0. Abscissa, distance along the longitudinal axis of the component fiber in millimeters. (See text.)

Fig. 7. The above mentioned internodal portions of $n = 1$ and 2 are shown. The potential decay of these portions is drawn as straight lines for convenience. It is of importance here to note that the value of Equation 2 for $x = 0$ is infinite, but in reality the potential at $x = 0$ has, of course, a limited value referred to as E_0. The intersection of the ordinate by the line expressed by Equation 3 for the subscript $n = 1$ gives the value of E_0.

When the tip of the current electrode applied intracellularly is much smaller than the fiber diameter, the curve of the actual potential distribution should have another concave curvature (not illustrated in the figure). It has a very steep configuration almost stuck to the ordinate for the very small values of x. This steeply falling portion of the curve represents a potential distribution attributable to the transverse effect around the tip of the current electrode (Hodgkin and Rushton, 1946; Katz, 1948), where the potential distribution

should be thought of as having a three dimensional spread. As the length constant in the present case is some fifty times as large as the fiber diameter, the range of x influenced by the transverse effect is very small as described above. The gradient of the potential decay along the axis of the fiber should be larger than that in the transverse direction, because there is a resistive barrier caused by the membrane in the transverse direction. The potential at the tip of the current electrode has a limited value, which mainly depends on the tip radius of the electrode (see Tip resistance in this section).

The model previously mentioned has, as it were, very large interstitial spaces. But this is not the case for the actual cardiac tissue. If one axis of the coordinate of the model, whether vertical or horizontal, is inclined so that the lattice is folded so that the meshes become very slender rhombi, then each pair of adjacent sides is almost touching. This model would simulate the actual cardiac tissue in a more plausible manner. The model modified in this way could give an account of the directional difference of the potential distribution of the tissue.

III. *Effective Resistance*

Any network of cables has an effective impedance inherent in its peculiar structure. Thus the analysis on the cardiac tissue would offer significant information on the structural geometry of the anastomosis. The effective resistance of the network at $x = 0$, R_0 is defined here as the ratio of potential at $x = 0$ to the total current through the membrane when the current is applied between a point inside the cable and the external medium. In the present case the resistance of interstitial space is assumed to be negligible.

For convenience of comparison, the following model is assumed; that is, a model of four half-infinite linear cables starting from a point at which the current is applied and without any other anastomosis. This might be considered as the ultimate reduction of our lattice model where the internodal distance is infinite. In this case R_0 is calculated from the well known formula for the linear cable

$$R_0 = \tfrac{1}{4}R_c = \tfrac{1}{4}\sqrt{r_i r_m} = \tfrac{1}{4}r_i\lambda$$

where R_c, the characteristic resistance, is R_0 of half-infinite linear cable. On the other hand the total membrane current of our lattice model is expressed as follows:—

$$I_0 = -\frac{4}{r_i}\left(\frac{dE_{0\sim 1}}{dx}\right)_{x=0}$$

so that the effective resistance, R_0, of the model can be calculated as

$$R_0 = \frac{1}{4} r_i \lambda \left(\frac{1}{\sinh \frac{d}{\lambda}} \left\{ \exp\left(\frac{d}{\lambda}\right) - \frac{K_0\left(\frac{d}{\lambda}\right)}{m} \right\} - 1 \right)^{-1} \tag{4}$$

where m is expressed as Equation A-7 in the Appendix, section II.

The value of R_0 in Equation 4 may vary with several parameters (R_i, R_m, a, and d), but attention is paid here mainly to the structural factors. The

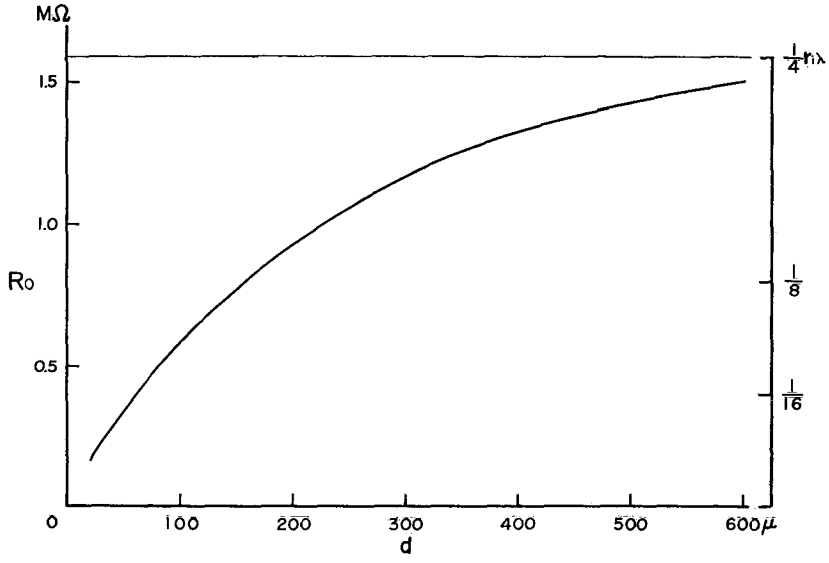

FIGURE 4. Relation between internodal distance and effective resistance. Abscissa, internodal distance of the fiber in micra. Left hand ordinate, effective resistance in MΩ. Right hand ordinate, structural factor as indicated in fraction multiplying $r_i\lambda$. The transverse straight line in the upper portion of the figure indicates the effective resistance of the four half-infinite linear model. (See text.)

relation between the internodal distance d and the effective resistance R_0 can be graphed as illustrated in Fig. 4. The transverse straight line in the upper portion of the figure shows the value of R_0 for the four half-infinite linear cable model. On the right hand ordinate one can easily compare the R_0 value for the lattice model to that of the reduced model for a given value of d. Parameters other than d in this calculation were the same as previously mentioned.

The fraction $(1/k)$ multiplying $r_i\lambda$ in the figure indicates a factor characteristic of the geometry of the anastomosis. Consequently, k indicates the ratio of the characteristic resistance or effective resistance of a half-infinite linear cable to that of a lattice.

In the case of the calculated example ($d = 100\ \mu$) k takes a value of 11, and this corresponds to R_0 of about 580 KΩ.

IV. *Coupling Resistance between Curent and Recording Electrodes*

When the electronic decay in the real tissue is measured experimentally by employing current and recording micropipettes placed close together, the data obtained might be distorted due to "resistive coupling" between the electrodes. The coupling resistance at the tip of the current electrode is referred to as tip resistance, $R_{t(L=0)}$. The so-called electrode resistance of a micropipette immersed in an electrolytic solution consists of two components, the resistance inside the electrode and the tip resistance in the medium.

The tip resistance $R_{t(L=0)}$ is expressed as follows on the assumption described in the Appendix, section III

$$R_{t(L=0)} = \frac{\rho}{2\pi c} \tag{5}$$

where, ρ is the specific resistance of the medium, and c is the radius of the tip of the micropipette. Generally, at any point in the medium the coupling resistance R_t to the indifferent electrode can be expressed as

$$R_t = \frac{\rho}{2\pi(2L + c)} \tag{6}$$

where L, is the distance between current and recording electrodes. Fig. 10A illustrates such an R_t-L relation in two kinds of solutions with different specific resistances calculated from Equation 6 in the case of the outer pipette of pencil type microelectrode with a constant tip diameter of 1 μ and a gradient of the inner surface of 15/100 (see Experimental method under Evidence). The upper curve indicates the R_t-L relation in NaCl-free Tyrode's solution (having a specific resistance of about seven times as large as that of normal Tyrode's). The lower curve shows the relation in normal Tyrode's solution. Each curve comprises two portions; i.e., the part illustrated in solid line is the distribution of the coupling resistance in the medium, and the part illustrated in broken line is the sum of the coupling resistance and the resistance of the electrode proper. The intraelectrode resistance is also calculated to have an ohmic resistance having the resistivity of 1 M KCl solution.

The differences in tip resistance on the same micropipette immersed in different media having specific resistances of ρ_1 and ρ_2 are calculated in the following equation

$$\Delta R_{t(L=0)} = \frac{\rho_1 - \rho_2}{2\pi c} \tag{7}$$

EVIDENCE

I. *Experimental Method*

MATERIAL AND SOLUTION The heart of an adult mouse was cut into pieces along the longitudinal axis. A piece of ventricle which scarcely showed spontaneous beats was selected, and mounted on a cork block immersed in the Tyrode solution equilibrated with a gas mixture of 95% O_2 and 5% CO_2. The temperature of the bath was kept at 35 ± 0.5°C.

Composition of the Tyrode solution used was as follows. NaCl 137 mM, KCl 2.6 mM, $CaCl_2$ 1.8 mM, $MgCl_2$ 0.5 mM, $NaHCO_3$ 11.7 mM, NaH_2PO_4 3.2 mM, glucose 5.6 mM.

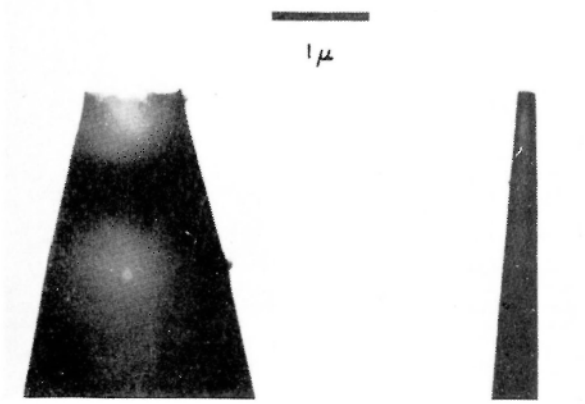

FIGURE 5. An electron micrograph of tips of outer and inner pipettes for superfine coaxial pencil type microelectrode. Left, outer pipette. Right, inner pipette.

ELECTROTONIC POTENTIAL ALONG THE FIBER A pair of intracellular microelectrodes filled with 3 M KCl (Ling and Gerard, 1949) were inserted into a superficial ventricular fiber of the preparation mounted epicardium up and slightly stretched to some 130% of the original length. One electrode was used for passing the current and the other for recording the potential.

Prior to application, under a high magnification microscope these two microelectrodes were set to the manipulator a certain distance apart. After the one insertion, the interelectrode distance was varied within the range of 25 to 200 μ by changing the position of the recording electrode, whereas the position of the current electrode was unchanged. Measurements were made for the interelectrode distances of 25, 50, 100, 150, and 200 μ (within ±10% of each distance). For the longer distances of 1 and 1.5 mm, these microelectrodes were mounted on two micromanipulators respectively and inserted independently in the fiber. The penetration of the membrane by electrodes was checked by the appearance of resting and action potentials for both electrodes. Then several measurements were made for each interelectrode distance. The data were treated statistically.

Hyperpolarizing currents of the order of approximately 10^{-8} to 10^{-7} amp lasting more than 200 msec were sent to the cell interior from a square pulse generator with

isolating unit through the current limiter (100 MΩ). The total current through the cell membrane was measured as the potential drop across the resistor of 10 KΩ inserted in the circuit. Membrane potential changes caused by the current flow were fed to a dc amplifier via a high input-impedance preamplifier (Tomita and Torihama, 1956).

The current and the potential obtained were observed and recorded simultaneously by a dual-beam oscilloscope and a long recording camera.

TRANSVERSE POTENTIAL Potential distribution in the transverse direction within a fiber was measured directly by means of a pencil type coaxial superfine microelectrode (PME) (Tomita and Kaneko, 1965). This type of electrode consisted of two micropipettes, arranged coaxially, whose tips were less than 1 and 0.2 μ diameter

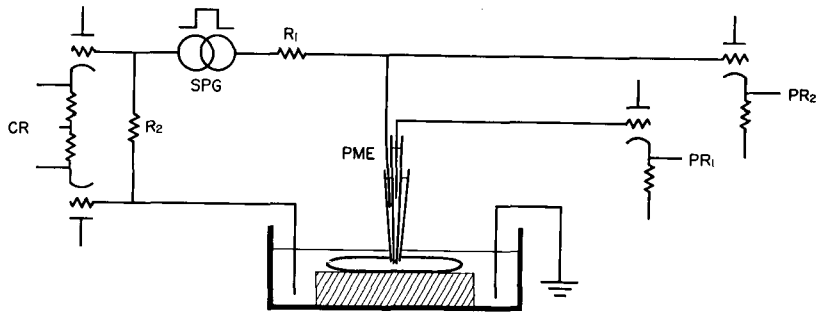

FIGURE 6. Experimental arrangement for pencil type microelectrode. *CR*, current recording. *PME*, pencil type microelectrode. PR_1 and PR_2, potential recordings for inner and outer pipettes. R_1, current limiter (100 MΩ). R_2, resistor across which the current was measured (10 KΩ). *SPG*, square pulse generator with isolating unit.

respectively. These were fine enough to be inserted into the cell interior of the ventricular fiber. An electron micrograph of the tips of two pipettes is shown in Fig. 5. The inner and outer pipettes were filled with 3 and 1 M KCl solution respectively. Before insertion the tips of both pipettes were adjusted so as to be flush. The penetration of the cell membrane with the coaxial electrode was checked by the appearance of resting and action potentials for both pipettes. The tip of the internal pipette could be extended along the axis of the electrode within the range of several micra, both tips being in the same fiber. The arrangement of the measurement is shown in Fig. 6.

After advancement of the internal pipette for a given distance, a square pulse of current was sent through the external pipette and the potential thus produced inside the fiber was picked up by the internal pipette.

II. *Experimental Results*

POTENTIAL DISTRIBUTION ALONG THE FIBER The recording and current electrodes were inserted into the superficial fibers on a line parallel to the fiber direction, and the interelectrode distance was varied from 25 μ to 1.5 mm. In this case, interelectrode distance indicates the actual length on the

fiber axis. Curve A of Fig. 8 shows the ratio of electrotonic potential E along the fiber to the total current applied I_0 against the distance x on the semilogarithmic coordinate, that is, E/I_0 is used in this case instead of E/E_0 which appeared under Theory, because E_0 could not be obtained directly from the

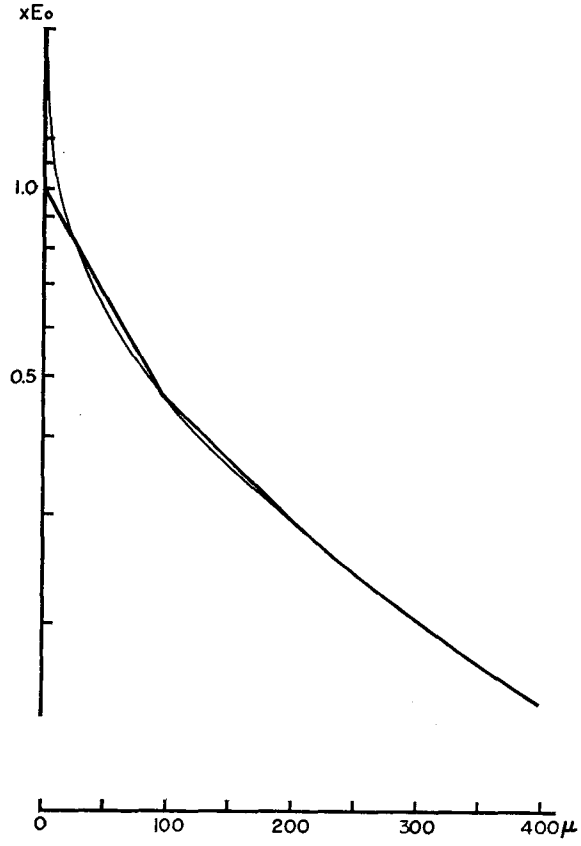

FIGURE 7. Enlargement of the tonic potential distribution near the origin. Light curve is that of the Bessel function in Fig. 3 and heavy one is the actual potential distribution in the lattice model. Note that the distribution for the internodal portions between 0 and 100 μ, and 100 μ and 200 μ is simply indicated by the bold straight lines on the semilogarithmic coordinate instead of the actual distribution expressed as Equation 3 in the text for convenience. (See text.)

experiment. An example of a series of records is shown in Fig. 9. In Fig. 8A for the distances larger than about 20 μ, there was no appreciable indication of discontinuity in the potential distribution along the fiber. Within a wide range of distances, the curve cannot be considered to be exponential. For large distances, the slope of the curve tended to decrease.

If it could be assumed that the curve for smaller x (less than 100 μ) were

linear and that the tissue had linear cable properties, the apparent length constant obtained from the gradient of such a portion would be about 70 μ. On the other hand, from the results of five series of measurements for sufficiently long interelectrode distances (1 and 1.5 mm), λ is approximately 400 to 700 μ on the same assumption. The theoretical length constant is 500 μ when primary parameters are chosen as indicated under Theory. The theoretical value of λ falls on the upper limit of the range of λ obtained from the experimental data shown in Fig. 8A, when assumptions are made that the actual distribution of electrotonic potential is expressed by Equation 2 and that d is

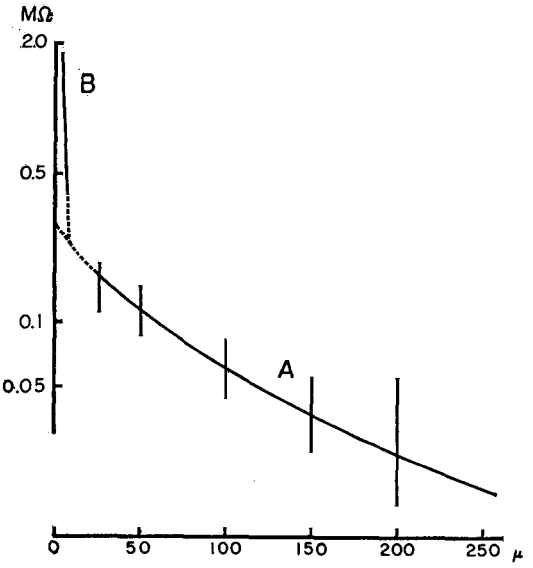

FIGURE 8. Electrotonic spread along the axis (curve *A*) and in the transverse direction (curve *B*) obtained from measurement. Abscissa, distance from current electrode in micra. Ordinate, tonic potential expressed as a ratio to total current applied in MΩ. Vertical lines indicate the range of distribution of approximately 7 to 10 measurements, and curve *A* is drawn from mean of measurements on each distance. Broken lines are those drawn by extrapolation of curves obtained experimentally. (See text.)

100 μ. This indicates that the value obtained by the theoretical calculation is reasonable. The distribution curve may well be fit to the theoretical one (illustrated in Fig. 7).

The effective resistance, R_0, obtained graphically by the extrapolation of curve A in Fig. 8 ranged from 200 to 600 KΩ (mean value, about 300 KΩ). This can be expressed in terms of the factor k (see Theory), whose value falls in the range of approximately 12 to 25. If fiber diameter a and electrical constants R_i, R_m are assumed to be the same as written under Theory, d should have the values of 30 to 110 μ as calculated from Equation 4. These values are included in the range of distribution of d obtained from histological examination. On the same assumption about the value of d, other parameters adopted for the theoretical calculation proved to be almost reasonable, although there is a tendency for the values of $r_i \cdot r_m$ and r_m/r_i in the theoretical calculations to be somewhat larger than those obtained from the experimental data shown in Fig. 8A.

POTENTIAL DISTRIBUTION IN TRANSVERSE DIRECTION The intracellular potential change caused by the current flow was also measured in the transverse direction within a single component fiber by means of a coaxial superfine microelectrode. After the tips of PME had been inserted into the cell interior, the inner pipette was advanced in steps of a few micra along the axis of the

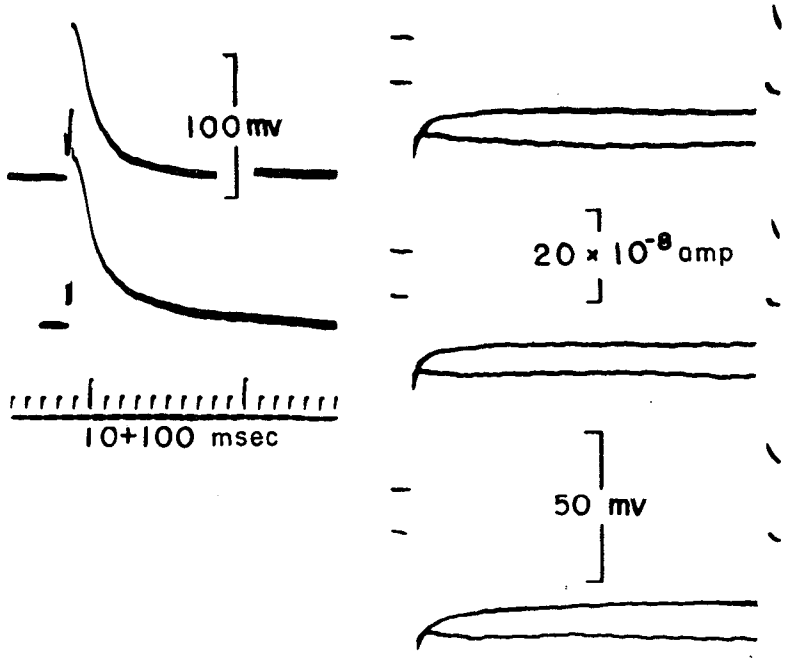

FIGURE 9. An example of a series of records in the experiment on the electrotonic potential along the fiber. Left, action potentials led simultaneously from recording (lower trace) and current electrode (upper trace) without circuit for passing the current. Resting potentials were about 80 to 90 mv. Right, simultaneous recording of electrotonic potential (E, lower trace) and total current through the membrane (I_0, upper trace) in various intensities. Interelectrode distance, 50 μ.

electrode and the potential for the constant current flow was recorded at each step. A typical example is shown in Fig. 8B. Although it was actually measured in the experiment in the transverse direction at $x = 0$ within a fiber, graphically it was plotted for the distance x along the fiber for convenience of comparison with A. The conversion of direction could be reasonably made at a site very close to the tip of the current electrode, since the potential distribution should be of three dimensional spread. More strictly, the gradient of the potential should be somewhat smaller in the transverse direction than in the longitudinal one (see Theory). The influence of the transverse effect on the tonic potential spread has an extent of the order of x shown in Fig. 8.

The gradient of curve B is much greater than that of curve A for the same range of x. Therefore, if the value of I_0 is known, the intersecting point of curve A and the ordinate gives the imaginary potential value (E_0) required for producing such a potential decay as that of curve A without any contamination of the transverse effect. The resistance to the external medium seen from the tip of the current electrode in a fiber; that is, the ratio of the potential caused by the current flow at the tip of the current electrode to the current intensity (I_0) was usually more than several MΩ. And yet, as seen here, the membrane resistance in this case is not high enough to establish the equipotentiality around the tip in the cell interior when the current is applied.

Thus, when an attempt is made to determine the electrical properties from the longitudinal potential distribution along the fiber, the transverse effect should be differentiated from the others.

COUPLING RESISTANCE When both tips of PME are flush and immersed in a solution, a considerably larger potential is developed from the inner pipette by passing the current through the outer one. This is due to tip resistance between both pipettes.

In the following description, the displacement of the tip of the inner pipette from that of the outer pipette along the axis is referred to as L, and the tips of both pipettes adjusted to be flush under the microscope are defined as $L = 0$. In the direction towards the stem of the outer pipette, L is positive. L is negative in the opposite direction (see inserted schema, Fig. 10). The coupling resistance at L, R_t, is defined as the ratio of the evoked potential at L to the applied current.

The inner pipette was shifted by steps of about 2.5 to 5 μ along the axis and at each position in either direction the current pulse of 3×10^{-7} amp in intensity was passed through the outer pipette employing the arrangement shown in Fig. 6.

Fig. 10B shows a typical case of R_t-L relations measured on one and the same PME for current in the direction from pipette to the medium. The lower curve was obtained in the normal Tyrode and the upper one in the glucose-Tyrode solution in which all NaCl was substituted by glucose. Reversal of current direction brought about essentially the same relation. In this figure, $L = 0$ is very close to the theoretical 0, since a point at which the first derivative of R with respect to L is maximum should be theoretically $L = 0$. In Tyrode's solution R_t was practically negligible at $L = -5$ μ. In glucose-Tyrode's solution there was a considerable R_t at a point where the displacement was more than 10 μ in the medium, and R_t was several times as large as normal Tyrode's solution for the same L. The curves resembled the corresponding ones in Fig. 10A obtained from the theoretical equations. This result shows that the coupling resistance can be reasonably considered on the theoretical basis as written in the previous section.

Theoretical values for positive L are the same even in different media. However, curves measured in normal Tyrode's and glucose-Tyrode's solutions are considerably different. This might be caused by diffusion between solutions and also by movement due to electroosmosis from passing current at the tip. Moreover, the movement of the solutions would be emphasized by extension and withdrawal of the inner pipette over the tip.

It is to be noted that the resistive coupling may be altered in different media and becomes larger for the larger electrode resistance. The specific resistance

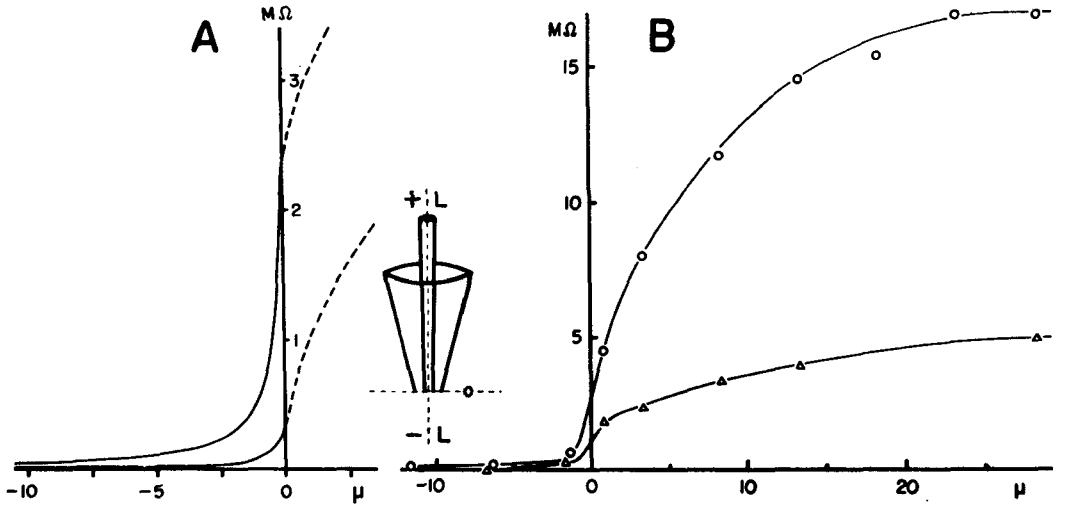

FIGURE 10. Distribution of coupling resistance between current and recording electrodes in relation to the interelectrode distance (L). Abscissa, distance from the tip of the current electrode towards the external medium (negative sign) and towards the stem of the electrode (positive sign) (see inserted schema). Ordinate, coupling resistance in MΩ. A, theoretical curves, upper curve, for the case of glucose-Tyrode's solution as the external medium, lower curve, for the case of normal Tyrode's solution. B, curves obtained from measurements, circles, glucose-Tyrode's solution; triangles, normal Tyrode's solution as external medium.

of the intracellular fluid is larger than that of Tyrode's solution. Thus, it would be expected that not only the coupling resistance but also the resistance inside the electrode might increase considerably in the cell interior when a high resistance electrode was used.

DISCUSSION

The model presented in this paper might be too simple compared with actual cardiac tissue. However, it is useful, as a working hypothesis, to know the tendency of the passive electrical properties of the tissue. There are many difficult problems in establishing the quantitative model. That is, parameters

related to the structure of the tissue are not accurately known, for (*a*) primary electrical constants R_i, R_m, and the resistance of the interstitial space, (*b*) values of a and d, and the mode of anastomosis of the fibers of the cardiac muscle, and (*c*) electrical properties of the intercalated disc.

Nevertheless, the lattice model proposed in the present study can simulate the actual cardiac tissue fairly well, as shown under Evidence. In our experiment the electrotonic spread of the potential to the neighboring cells could easily be observed. Thus, the resistance of the intercalated discs to the current spread to the neighboring cells would not be so large. This would support the local circuit theory for the conduction of excitation in cardiac tissue.

In the following paragraphs, some particular problems will be discussed.

The Model and Actual Tissue The significant differences in the mode of anastomosis between the model and the actual tissue are: (*a*) The fiber in the two dimensional model branches in the course of its run into three arms at each nodal point, whereas the real fiber usually bifurcates irregularly, (*b*) a fiber of the model connects with only two other fibers through the first order branch, but this would not always be the case for the actual cardiac tissue.

A modification is possible, in which alternate sides can be omitted from the lattice so that the resultant structure has bifurcations at every nodal point. In this modification the potential distribution with distance can be formulated in essentially the same manner (George, 1961), i.e. by a Bessel function and when the parameters are chosen appropriately, the distribution can be calculated to be the same except for minor differences close to the current source.

In the model previously mentioned two dimensional spread is considered. However, preparations from the ventricle should be taken to be of three dimensional spread. The extension of the lattice model to the three dimensional one is, of course, possible, but the mathematical treatment is more complicated. In this case, the manner of decay is also a Bessel functionlike curvature. Therefore, the two dimensional lattice model could be adopted qualitatively as representative of the models mentioned above. The effective resistance in real tissue might have a value between those in the two modified models. Hence, for quantitative calculation of R_0, the lattice model would be more suitable than the other two.

There is a directional difference of tonic decay in the atrium as reported by Woodbury and Crill (1961). This would be expected in the ventricle as well, because the tonic potential could spread in the axial direction of the fiber. The folded lattice model would give an account of this directional difference as already mentioned under Theory.

Decay of the Tonic Potential Exponential decay of the tonic potential in the unbranched Purkinje fiber has been reported by Weidmann (1952). On the other hand, the electrotonic spread in the cardiac tissue which has a syn-

cytial structure was shown not to be exponential (Matsuda, on the terminal Purkinje fiber; Woodbury and Crill, on the atrium). This was also confirmed in the present work. In these cases the gradients of potential decay with distance are larger at smaller values of x than those of exponential decay. But for larger distances the gradients become smaller and the curve of the potential distribution should be approximately exponential when a certain range of x is adopted. Practically, a reasonable value of λ could be obtained from the gradient for the whole range of the distance. The difference between apparent λ obtained in such a way and λ as defined under Theory can be obtained from the theoretical treatment, and it decreases as x becomes larger and when x is more than 1 mm, the difference is less than 10%. The value of λ which is obtained by the extrapolation of the curve with a gradient for the sufficiently large x is reasonable.

Matsuda (1960) suggested that the rapid decay for distances less than about 100 μ from the current electrode is due to the transverse effect in the special structure of terminal Purkinje fibers which are made up of approximately 8 to 10 fibers aggregated to form a discrete unit of about 100 to 120 μ in size. A similar deviation from the exponential decay for the smaller distances was also found in the atrium (Woodbury and Crill, 1961). These authors attributed this deviation to the two dimensional spread in the atrium which they assumed to be a simplified conductive plane with resistive membranes. Such a rapid decay of potential spread was observed in the ventricular working muscle as well in the present study. According to our histological examination, however, any special structure which would cause the very rapid decay of tonic potential was not observed except for the ordinary branching of syncytial structure. Based on this observation, it may be concluded that the Bessel functionlike decay of potential spread is due to the ordinary syncytial network of the cardiac tissue.

Nevertheless, our results show that the effective resistance (R_0) of the ventricular muscle is less than several hundred kiloohms. This value is equivalent to that of a point from which more than ten component fibers of infinite extent branched; i.e., the factor k defined under Theory is approximately 12 to 25. k calculated from Matsuda's data is about 15 and this value seems to be deduced from the simple syncytial network without fiber aggregations. In the present experiment, as predicted from the ratio of the diameter to the length constant, the range in which the transverse effect could be observed was small. When the parameters under Theory are adopted, the resistance per unit area of intercalated disc can be calculated to be approximately 500 to 2000 times lower than that of the fiber membrane, and the upper limit of disc resistance per unit area is $2\Omega \cdot cm^2$. This calculation is derived from the assumption that the cell length is approximately 50 to 200 μ and that the internal resistance of the fiber is lumped to intercalated discs. This value for

disc resistance is in good agreement with that calculated from the electrical measurements on rat atrium by Woodbury and Crill (1961) and also with the potassium component of disc resistance obtained from K^{42}-diffusion experiments on sheep ventricle by Weidmann (1964).

Transverse Effect and Tip Resistance With the aid of PME, the transverse potential decay at $x = 0$ was measured and it was inferred that the range in which the effect has a significant influence on the tonic potential decay in the longitudinal direction is as small as expected from the theoretical consideration.

The resistance at and around the tip of the current electrode to the indifferent electrode which was inserted into the fiber would depend not only upon the cellular factors but also upon the tip resistance. This tip resistance would be altered in different media, especially when the tip diameter was relatively small, even if the electrode resistance inside were unchanged (cf. Equation 7 under Theory).

When they compared the tonic potential around the tip and at sufficiently large distances from the current electrode, Sperelakis, Hoshiko, and Berne (1960) and Tarr and Sperelakis (1964) concluded that the tonic spread was discontinuous along the fiber. They ascribed this discontinuity to the relatively large resistance of the intercalated discs. However, our measurements never revealed the discontinuity along the fibers except for the very rapid potential decay around the current electrode as shown in Fig. 8B. In other words, even within one cell which was impaled with the current electrode, there was at first a steep potential decay and then a gentle spread continuously to the neighboring cells. This means that it is not necessary to assume a high value of resistance for the intercalated discs. The conclusion of these authors seems to come from the fact that the high input resistance obtained was taken for the true value of R_0 in calculation.

Generally, with a single microelectrode and also with a double barreled microelectrode it is impossible to obtain the effective resistance R_0 quantitatively by subtracting the resistance measured in the extracellular medium from that obtained intracellularly. Even when two microelectrodes are employed, it is also impossible to obtain the exact electrotonic potential free from the effect of coupling resistance around the tip of the current electrode. The value of resistance obtained by such subtraction is always much larger than the true value of R_0. This error cannot be neglected as the membrane resistance is usually not so high compared with the tip resistance.

APPENDIX

I. *Derivation of Differential Equation of E*

If the number of the sides between $(n - 1)$th and nth nodal point is expressed as N at n, N is a function of n. The total internal and membrane resistances per unit

length at n are

$$\left.\begin{aligned} f_i(n) &= \frac{r_i}{4n} \\ f_m(n) &= \frac{r_m}{4n} \end{aligned}\right\} \tag{A-1}$$

where $n = x/d$, and when current is applied at $n = 0$, the node n will all be at the same potential. An assumption is made that Equations A-1 can hold for all values of $x\,(0 < x < +\infty)$; i.e., a new model in which $n\,(= x/d)$ is of continuous nature is presented as an approximation. Then a set of differential equations can be assumed as follows:—

$$\left.\begin{aligned} -\frac{dE}{dx} &= I \times f_i(x) \\ -\frac{dI}{dx} &= E \times \frac{1}{f_m(x)} \end{aligned}\right\} \tag{A-2}$$

Eliminating I from Equations A-2, the following differential equation can be obtained,

$$\frac{d^2E}{dx^2} + \frac{1}{x} \cdot \frac{dE}{dx} - \frac{1}{\lambda^2} \cdot E = 0 \tag{A-3}$$

This is Equation 1 under Theory. The general solution of Equation A-3 is

$$E = AK_0\left(\frac{x}{\lambda}\right) + BI_0\left(\frac{x}{\lambda}\right)$$

where A and B are constants and

$$I_0\left(\frac{x}{\lambda}\right) = 1 + \frac{(x/\lambda)^2}{2^2} + \frac{(x/\lambda)^4}{2^2 \cdot 4^2} + \frac{(x/\lambda)^6}{2^2 \cdot 4^2 \cdot 6^2} + \cdots$$

$$K_0\left(\frac{x}{\lambda}\right) = (\log 2 - \gamma) \cdot I_0\left(\frac{x}{\lambda}\right) - \left\{ I_0\left(\frac{x}{\lambda}\right) \cdot \log\left(\frac{x}{\lambda}\right) - \frac{(x/\lambda)^2}{4} - \cdots \right\}$$

in which γ is Euler's constant having a value of $0.5772 \cdots$.

When x is infinite, E is zero, so B should be zero. Therefore

$$E = AK_0\left(\frac{x}{\lambda}\right) \tag{A-4}$$

This also appeared under Theory (Equation 2).

II. *Determination of* α

As already mentioned, at internodal portions in the lattice model, the potential dis-

tribution along the longitudinal axis of the fiber should be exponential. So within the ranges from 0 to 1, and 1 to 2 of n, E is related to x by the following equations

$$\left.\begin{aligned} E_{0\sim1} &= A_1 \exp\left(-\frac{x}{\lambda}\right) + B_1 \exp\left(\frac{x}{\lambda}\right) \\ E_{1\sim2} &= A_2 \exp\left(-\frac{x}{\lambda}\right) + B_2 \exp\left(\frac{x}{\lambda}\right) \end{aligned}\right\} \tag{A-5}$$

On the other hand, E at $x = 0$ is E_0 and values at $x = d$ and $2d$ are given by Equation A-4. Therefore one can eliminate constants A_1, B_1, A_2, and B_2 from Equations A-5 to express them in terms of A, d, λ as well as E_0, and then calculate the derivatives of Equations A-5 at $x = d$ ($n = 1$).

At the nodal point $n = 1$, the current flowing in and that flowing out inside the fiber should be equal, so the following equation is obtained

$$\left(\frac{dE_{0\sim1}}{dx}\right)_{x=d} = 3\left(\frac{dE_{1\sim2}}{dx}\right)_{x=d} \tag{A-6}$$

From Equation A-6,

$$A = \frac{E_0}{m}$$

where

$$m = 2K_0\left(\frac{d}{\lambda}\right) \cdot \exp\frac{d}{\lambda}\left(\exp -\frac{2d}{\lambda} + 1\right) - 3K_0\left(\frac{2d}{\lambda}\right) \tag{A-7}$$

On the other hand E_0 has, as mentioned previously, a limited value and so it is expressed as follows:—

$$E_0 = AK_0\left(\frac{\alpha}{\lambda}\right)$$

So,

$$K_0\left(\frac{\alpha}{\lambda}\right) = m$$

α is expressed so as to have a very small value at the point close to the origin. The values of α and m, when $d = 100\ \mu$ and $\lambda = 500\ \mu$, are calculated to be about 1.3×10^{-3} cm and 3.9 respectively.

III. *Calculation of Coupling Resistance*

Assuming that the cross-sectional area at the electrode tip, whose radius is c, is equivalent to the surface of a sphere which has a radius of $c/2$, the resistance at the surface to

infinity in the medium ($R_{t(l=c/2)}$) is expressed as follows (Tomita and Kaneko, 1965):—

$$R_{t(l=c/2)} = \int_{c/2}^{\infty} \frac{\rho\, dl}{4\pi l^2} = \frac{\rho}{2\pi c}$$

where l is the distance from the center of the sphere in the medium, ρ is the specific resistance of the external medium, and it is assumed to be ohmic resistance.

And R_t can be generally expressed as follows:—

$$R_t = \frac{\rho}{2\pi c} - \int_{c/2}^{l} \frac{\rho\, dl}{4\pi l^2} = \frac{\rho}{4\pi l}$$

In projecting the assumed system written above to the real system of electrode and external medium as a whole, the surface at the tip of the electrode should correspond to the spherical plane of $l = c/2$ in the external medium. Therefore, the following equations are more suitable to express the system (Tanaka, Sasaki, and Ogino, 1963)

$$R_{t(L=0)} = \frac{\rho}{2\pi c} \tag{A-8}$$

$$R_t = \frac{\rho}{2\pi(2L + c)} \tag{A-9}$$

where L is the distance from the spherical surface and expressed as $L = l - c/2$ and R_t in these equations is the resistance for L; that is, the coupling resistance in the external medium. Equations A-8 and A-9 correspond respectively to Equations 5 and 6 under Theory.

We are greatly indebted to Dr. T. Tomita, Keio University School of Medicine, for his valuable suggestions and technical cooperation with the pencil type microelectrode. We also wish to express our thanks to Drs. T. Tosaka, T. Hojo, and T. Ogino for their assistance throughout the experiments, and to Dr. L. G. Bishop, California Institute of Technology, and Dr. R. Kikuchi for suggesting some changes in wording.

This work was supported by a Scientific Research Grant for 1963 from the Ministry of Education of Japan.

Received for publication 28 May 1965.

REFERENCES

GEORGE, E. P., Resistance values in a syncytium, *Australian J. Exp. Biol.*, 1961, **39**, 267.

HODGKIN, A. L., and RUSHTON, W. A. H., The electrical constants of crustacean nerve fibre, *Proc. Roy. Soc. London, Series B*, 1946, **133**, 444.

KATZ, B., The electrical properties of the muscle fibre membrane, *Proc. Roy. Soc. London, Series B*, 1948, **135**, 506.

LING, G., and GERARD, R. W., The normal membrane potential of frog sartorius fibres, *J. Cell. and Comp. Physiol.*, 1949, **34**, 383.

MATSUDA, K., Some electrophysiological properties of terminal Purkinje fibers of

heart, *in* Electrical Activity of Single Cells, (Y. Katsuki, editor), Tokyo, Igakushoin, 1960, 283.

SPERELAKIS, N., HOSHIKO, T., and BERNE, R. M., Nonsyncitial nature of cardiac muscle: membrane resistance of single cells, *Am. J. Physiol.*, 1960, **198,** 531.

TANAKA, I., SASAKI, Y., and OGINO, T., Pencil type superfine microelectrode technique (in Japanese), *Igaku No Ayumi*, 1963, **47,** 47.

TARR, M., and SPERELAKIS, N., Weak electrotonic interaction between contiguous cardiac cells, *Am. J. Physiol.*, 1964, **207,** 691.

TOMITA, T., and KANEKO, A., An intracellular coaxial microelectrode—Its construction and application, *Med. Electron. Biol. Eng.*, 1965, **3,** 367.

TOMITA, T., and TORIHAMA, Y., Further study on the intraretinal action potentials and on the site of ERG generation, *Japan. J. Physiol.*, 1956, **6,** 118.

WEIDMANN, S., The electrical constants of Purkinje fibres, *J. Physiol.*, 1952, **118,** 348.

WEIDMANN, S., Electrophysiologie der Herzmuskeltaser, (zweite neubearbeitet Auflage), Bern, Hans Huber, translated into Japanese by K. Matsuda, Kyoto, Kimpodo, 1957.

WEIDMANN, S., The functional significance of the intercalated discs, *in* Electrophysiology of the Heart, (B. Taccardi and G. Marchetti, editors), Oxford, Pergamon Press, 1964, 149.

WOODBURY, J. W., and CRILL, W. E., On the problem of impulse conduction in the atrium, *in* Nervous Inhibition, (E. Florey, editor), Oxford, Pergamon Press, 1961, 124.